Molecular Crystals and Liquid Crystals Science and Technology. Section A. Molecular Crystals and Liquid Crystals
Publication details, including instructions for authors and subscription information:
http://www.tandfonline.com/loi/gmcl19

Characteristics of C1 and C2 States in Surface-Stabilized Ferroelectric Liquid Crystals with Chevron Layer Structure

Tadashi Akahane [a] , Hiroshi Tamura [a] & Munehiro Kimura [a]
[a] Department of Electrical Engineering, Faculty of Engineering, Nagaoka University of Technology, Kamitomioka 1603, Nagaoka, Niigata, 940-21, Japan
Version of record first published: 23 Sep 2006.

To cite this article: Tadashi Akahane , Hiroshi Tamura & Munehiro Kimura (1995): Characteristics of C1 and C2 States in Surface-Stabilized Ferroelectric Liquid Crystals with Chevron Layer Structure, Molecular Crystals and Liquid Crystals Science and Technology. Section A. Molecular Crystals and Liquid Crystals, 263:1, 233-244

To link to this article: http://dx.doi.org/10.1080/10587259508033588

Mol. Cryst. Liq. Cryst. 1995, Vol. 263, pp. 233–244
Reprints available directly from the publisher
Photocopying permitted by license only

CHARACTERISTICS OF C1 AND C2 STATES IN SURFACE-STABILIZED FERROELECTRIC LIQUID CRYSTALS WITH CHEVRON LAYER STRUCTURE

Tadashi AKAHANE, Hiroshi TAMURA and Munehiro KIMURA

Department of Electrical Engineering, Faculty of Engineering,
Nagaoka University of Technology,
Kamitomioka 1603, Nagaoka, Niigata 940-21 Japan

Abstract Characteristics of the dynamic response of the surface-stabilized ferroelectric liquid crystals (SSFLC) in the C1 and C2 states to an electric field is investigated by means of simulations based on the continuum theory of SmC* phase. The effects of the surface pretilt on them are discussed. The effects of dielectric anisotropy are also studied.

1 Introduction

Since the X-ray study on surface stabilized ferroelectric liquid crystals (SSFLCs) by Rieker *et al.*,[1] it is well established that the chevron layer structure is quite common in homogeneously aligned cells of ferroelectric SmC* liquid crystals independent of surface treatment. The experiments suggest that the chevron interface is extremely sharp, and that the region of layer bend can effectively be regarded as a surface.[2]

When the finite surface pretilt exists at the substrates, C1 and C2 states are distinguished depending on the relationship between the direction of the chevron kink and the direction of the surface pretilt.[3] Two stable molecular orientations are possible in each of the C1 and C2 states, the uniform state and the twisted (splayed) state. Therefore, four states, C1U (C1-uniform), C1T (C1-twisted), C2U (C2-uniform) and C2T (C2-twisted) may be distinguished. Indeed, Itoh *et.al.* observed these four states in an SSFLC cell with low pretilt aligning films.[4]

We formulated the basic equations to simulate the dynamic response of SSFLCs with chevron layer structure to an applied voltage, in general manner, including the effect of polarization electric field and dielectric anisotropy, based on $\boldsymbol{c}$-director expression of the elastic free energy density.[5] Based on this formalism, we calculated the polarization reversal current under triangular wave voltages,[5] and switching characteristics under pulsed voltages[6] in the case of C1 state.

In this study, we present the switching characteristics both of the C1 and C2 states in SSFLCs and compare them. In particular, we investigate the effects of surface anchoring conditions and dielectric anisotropy on them.

2 Basic Equations

The symmetric chevron layer structure is modeled into such one that the layers are uniformly tilted, in the opposite sense, above and below a planar interface (chevron interface) situated midway between the bounding plates. In the C1 state, the layer tilt angles in the upper half and in the lower half of the cell are $\Psi^{\mathrm{U}} = \Psi$, and $\Psi^{\mathrm{L}} = -\Psi$, respectively. In the C2 state, the layer tilt angle takes opposite sign to the C1 state (see Fig.1). We take the Y-axis along the cell normal, Z-axis along the direction of the projection of the layer normal in the bounding plate, and X-axis perpendicular to both $\boldsymbol{Y}$ and $\boldsymbol{Z}$. The lower bounding plate and the upper bounding plate are located at $Y = 0$ and $Y = d$, respectively (the cell thickness is d). The chevron interface is thus located at $Y = d/2$. The local xyz-coordinate system is defined such that the z-axis is along the layer normal, x-axis is parallel to $\boldsymbol{X}$, and y-axis is perpendicular both to $\boldsymbol{z}$ and $\boldsymbol{x}$. Therefore, the xyz-coordinate system is transformed into the laboratory XYZ-coordinate system by rotation of the angle Ψ^{U} or Ψ^{L} about the x-axis, depending on the upper half or the lower half of the cell.

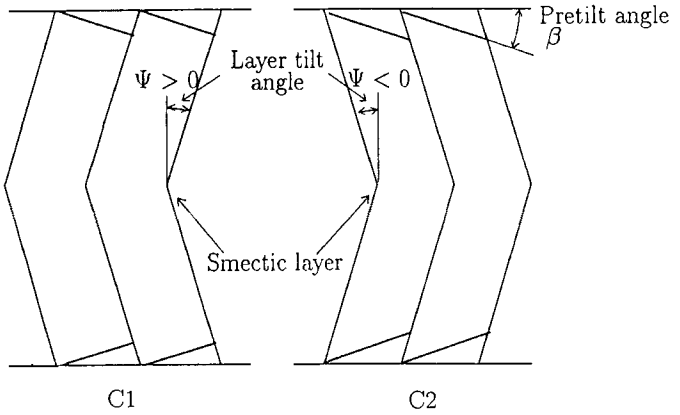

Fig.1 Layer structures of C1 and C2 states.

The layer normal $\boldsymbol{k}$, the c-director $\boldsymbol{c}$, the unit vector along the spontaneous polarization $\boldsymbol{p}$, and the n-director $\boldsymbol{n}$ in the XYZ-coordinate system are given by

$$\begin{cases} \boldsymbol{k} &= (0, -\sin\Psi, \cos\Psi), \\ \boldsymbol{c} &= (\cos\Phi, \cos\Psi\sin\Phi, \sin\Psi\sin\Phi), \\ \boldsymbol{p} &= (-\sin\Phi, \cos\Psi\cos\Phi, \sin\Psi\cos\Phi), \\ \boldsymbol{n} &= (\sin\theta\cos\Phi, \cos\Psi\sin\theta\sin\Phi - \sin\Psi\cos\theta, \\ & \quad \sin\Psi\sin\theta\sin\Phi + \cos\Psi\cos\theta), \end{cases} \tag{1}$$

where θ is the molecular tilt angle, Φ is the azimuthal angle of the c-director measured from x-axis and Ψ is the representative of Ψ^{U} or Ψ^{L}. The angle α between n-director and the bounding plane (hereafter, we call this angle out-of-plane tilt angle) is given by

$$\sin\alpha = n_Y = \cos\Psi\sin\theta\sin\Phi - \sin\Psi\cos\theta. \tag{2}$$

Therefore, the azimuthal angle where n-director is parallel to the bounding plate is given by

$$\sin\Phi = \tan\Psi/\tan\theta. \tag{3}$$

The angle δ between Z-axis and the projection of n-director on the bounding plate (hereafter, we call this angle in-plane tilt angle) is given by

$$\tan\delta = \frac{n_X}{n_Z} = \frac{\sin\theta\cos\Phi}{(\sin\Psi\sin\theta\sin\Phi + \cos\Psi\cos\theta)}. \tag{4}$$

If the layer structure does not change, the elastic free energy density f_{elas} of a chiral smectic C liquid crystal is given by[7)]

$$\begin{aligned} f_{\mathrm{elas}} &= \frac{1}{2}B_1\{\boldsymbol{k}\cdot(\boldsymbol{\nabla}\times\boldsymbol{c})\}^2 + \frac{1}{2}B_2(\boldsymbol{\nabla}\cdot\boldsymbol{c})^2 + \frac{1}{2}B_3\{\boldsymbol{c}\cdot(\boldsymbol{\nabla}\times\boldsymbol{c})\}^2 \\ &\quad -B_{13}\{\boldsymbol{k}\cdot(\boldsymbol{\nabla}\times\boldsymbol{c})\}\{\boldsymbol{c}\cdot(\boldsymbol{\nabla}\times\boldsymbol{c})\} \\ &\quad +D_1\{\boldsymbol{k}\cdot(\boldsymbol{\nabla}\times\boldsymbol{c})\} - D\{\boldsymbol{c}\cdot(\boldsymbol{\nabla}\times\boldsymbol{c})\}. \end{aligned} \tag{5}$$

We consider the one-dimensional problem where azimuthal angle Φ depends only on Y. Then, substitution of eq.(1) into eq.(5) leads to

$$\begin{aligned} f_{\mathrm{elas}} = \ & \tfrac{1}{2}\{(B_1\sin^2\Phi + B_2\cos^2\Phi)\cos^2\Psi + B_3\sin^2\Psi \\ & -2B_{13}\sin\Psi\cos\Psi\sin\Phi\}\Phi_{,Y}^2 \\ & +D_1\Phi_{,Y}\cos\Psi\sin\Phi - D\Phi_{,Y}\sin\Psi\ , \end{aligned} \tag{6}$$

where $\Phi_{,Y} = d\Phi/dY$. The D_1 term can be transformed into the surface energy term which plays the same role as polar surface anchoring . The D term can also be transformed into the surface energy term. This term disappears, however, in the case of a bookshelf layer structure ($\Psi = 0$) in contrast to the D_1 term.

When an electric field is applied along Y-axis, the dielectric free energy density f_{d} is given by

$$f_{\mathrm{d}} = -\frac{1}{2}\boldsymbol{D}\cdot\boldsymbol{E} = -\frac{1}{2}\varepsilon_{YY}E_Y^2 = -\frac{1}{2}\varepsilon_{YY}\phi_{,Y}^2\ , \tag{7}$$

where ϕ is an electric scalar potential, and ε_{YY} is the YY-component of the dielectric tensor. If the principal dielectric constants along $\boldsymbol{n}$, $\boldsymbol{p}$, and $\boldsymbol{p}\times\boldsymbol{n}$ are ε_3, ε_2,

and ε_1, respectively, ε_{YY} is given by

$$\begin{aligned}\varepsilon_{YY} &= \varepsilon_1(\cos\theta\sin\Phi\cos\Psi+\sin\theta\sin\Psi)^2+\varepsilon_2\cos^2\Phi\cos^2\Psi \\ &\quad +\varepsilon_3(\sin\theta\sin\Phi\cos\Psi-\cos\theta\sin\Psi)^2 \\ &= \varepsilon_2+\Delta\varepsilon(\sin\theta\sin\Phi\cos\Psi-\cos\theta\sin\Psi)^2 \\ &\quad -\partial\varepsilon(\sin^2\Phi\cos^2\Psi+\sin^2\Psi) \end{aligned} \tag{8}$$

where the dielectric anisotropies $\Delta\varepsilon=\varepsilon_3-\varepsilon_1$ and $\partial\varepsilon=\varepsilon_2-\varepsilon_1$.

The coupling energy density $f_{\rm p}$ between spontaneous polarization $\boldsymbol{P}_{\rm s}$ and an electric field is given by

$$f_{\rm p}=-\boldsymbol{P}_{\rm s}\cdot\boldsymbol{E}=-P_{\rm s}E_Y\cos\Psi\cos\Phi=P{\rm s}\phi_{,Y}\cos\Psi\cos\Phi\ . \tag{9}$$

We assume that the surfaces of bounding plates are homogeneous and characterized by the surface-anchoring energy per unit area $f_{\rm s}$ given by

$$\begin{cases} f_{\rm s}^0 &= \gamma_1^0(\sin\alpha^0-\sin\beta^0)^2-\gamma_2^0(\boldsymbol{p}^0\cdot\boldsymbol{S}^0)+\gamma_3^0\sin^2\delta^0 \text{ (lower surface)} \\ f_{\rm s}^d &= \gamma_1^d(\sin\alpha^d-\sin\beta^d)^2-\gamma_2^d(\boldsymbol{p}^d\cdot\boldsymbol{S}^d)+\gamma_3^d\sin^2\delta^d \text{ (upper surface)} \end{cases} \tag{10}$$

where superscripts 0 and d indicate the values at the lower and the upper bounding plates, respectively. In eq.(10), $\alpha^{0,d}$, $\beta^{0,d}$ and $\delta^{0,d}$ are the out-of-plane tilt angle, the pretilt angle and the in-plane tilt angle, at the lower or upper substrate, respectively. $\boldsymbol{S}^{0,d}$ is the inward normal of the lower or upper substrate and $\boldsymbol{S}^d=-\boldsymbol{S}^0$.

The first and the third terms in eq.(10) represent nonpolar anchoring and symmetric functions of the azimuthal angle of c-director Φ about $\Phi=\pm\pi/2$, as should be. The second term represents polar anchoring and breaks the symmetry mentioned above.

If we denote the n-director at the upper side of the chevron interface as $\boldsymbol{n}^{\rm U}$, and that at the lower side of the chevron interface as $\boldsymbol{n}^{\rm L}$, the orientation of $\boldsymbol{n}$-director is considered to be more stable with smaller angle χ between $\boldsymbol{n}^{\rm U}$ and $\boldsymbol{n}^{\rm L}$. Therefore, the energy of the chevron interface $f_{\rm i}$ is assumed to be given by

$$f_{\rm i}=-\gamma_{\rm c}\cos^2\chi=-\gamma_{\rm c}(\boldsymbol{n}^{\rm U}\cdot\boldsymbol{n}^{\rm L})^2\ . \tag{11}$$

As $\Psi^{\rm U}=\Psi$ and $\Psi^{\rm L}=-\Psi$, we obtain from eq.(1)

$$\begin{aligned} f_{\rm i} = &-\gamma_{\rm c}\{\sin^2\theta\cos\Phi^{\rm U}\cos\Phi^{\rm L}+\cos2\Psi\sin^2\theta\sin\Phi^{\rm U}\sin\Phi^{\rm L} \\ &+\tfrac{1}{2}\sin2\Psi\sin2\theta(\sin\Phi^{\rm U}-\sin\Phi^{\rm L})+\cos2\Psi\cos^2\theta\}^2\ . \end{aligned} \tag{12}$$

If we define

$$\begin{aligned} f_{\rm B} &= f_{\rm elas}+f_{\rm d}+f_{\rm p}\ , \\ f_{\rm S} &= f_{\rm s}^0\delta(Y)+f_{\rm s}^d\delta(Y-d)+f_{\rm i}\delta(Y-d/2)\ , \end{aligned}$$

the total energy per unit area of the cell is given by

$$F=\int_0^d(f_{\rm B}+f_{\rm S})\,dY\ . \tag{13}$$

In eq.(13), $f_{\rm B}$ is the bulk free energy density and $f_{\rm S}$ is related to the surface

anchoring energies including the chevron interface.

Introducing the rotational viscosity coefficient λ, the torque balance equation can be written as

$$\lambda \frac{\partial \Phi}{\partial t} = -\frac{\delta F}{\delta \Phi} . \tag{14}$$

From eq.(14), we obtain

$$\lambda \frac{\partial \Phi}{\partial t} = -\frac{\partial f_{\rm B}}{\partial \Phi} + \frac{\partial}{\partial Y}\frac{\partial f_{\rm B}}{\partial \Phi_{,Y}} \quad \text{(in the bulk)} , \tag{15}$$

$$\left(\frac{\partial f_{\rm B}}{\partial \Phi_{,Y}}\right)_{Y=0} = \frac{\partial f_{\rm s}^{0}}{\partial \Phi^{0}} \quad \text{(at the lower substrate)} , \tag{16}$$

$$\left(\frac{\partial f_{\rm B}}{\partial \Phi_{,Y}}\right)_{Y=d} = -\frac{\partial f_{\rm s}^{d}}{\partial \Phi^{d}} \quad \text{(at the upper substrate)} , \tag{17}$$

$$\left(\frac{\partial f_{\rm B}}{\partial \Phi_{,Y}}\right)_{Y=d/2-0} = -\frac{\partial f_{\rm i}}{\partial \Phi^{\rm L}} \quad \text{(at the lower side of chevron)} , \tag{18}$$

$$\left(\frac{\partial f_{\rm B}}{\partial \Phi_{,Y}}\right)_{Y=d/2+0} = \frac{\partial f_{\rm i}}{\partial \Phi^{\rm U}} \quad \text{(at the upper side of chevron)} . \tag{19}$$

In eqs.(16)-(19), we use the static approximation for the surface torque balance equations[8,9].

The scalar potential ϕ can be determined from $\delta F/\delta \phi = 0$, i.e.,

$$\frac{\partial}{\partial Y}\frac{\partial f_{\rm B}}{\partial \phi_{,Y}} = 0 . \tag{20}$$

From eq.(20),we obtain

$$\frac{\partial}{\partial Y}\{\varepsilon_{YY}\phi_{,Y}\} = \mathrm{div}\boldsymbol{P}_{\rm s} = -P_{\rm s}\cos\Psi\sin\Phi\frac{\partial \Phi}{\partial Y} \tag{21}$$

where $-\mathrm{div}\boldsymbol{P}_{\rm s}$ is the polarization charge. However, when the spontaneous polarization is not very large (strictly speaking the parameter $\Lambda = (P_{\rm s}d)^2/(B_2\varepsilon)$ is not very large)[10], the effect of polarization electric field due to this term is not very notable.[9] Therefore, we neglect this term in the following. Even in this case, ϕ is not a linear function of Y and an electric field is not constant through the cell because ε_{YY} depends on $\Phi(Y)$.

3 Numerical Results and Discussion

3.1 *Anchoring Function and Memory States*

First of all, let us investigate the stable alignment at the bounding plates and the chevron interface. We assume that two bounding plates are equally treated and $\gamma_1^0 = \gamma_1^d$, $\gamma_2^0 = \gamma_2^d$ and $\gamma_3^0 = \gamma_3^d$. We also assume that the cell is fabricated such that the rubbing directions of two plates are parallel. Then, the pretilt angle $\beta^d = -\beta^0$.

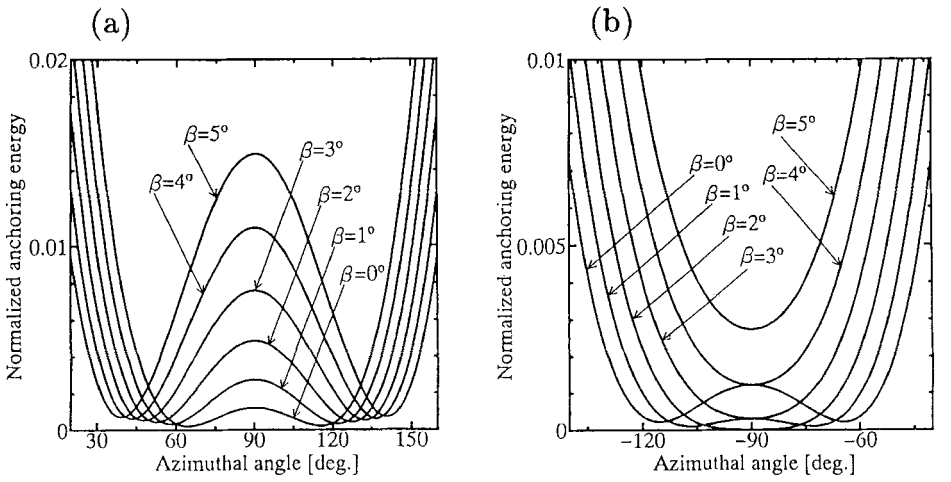

Fig.2 Normalized surface anchoring energy f_s^d/γ_1^d of the upper substrate. $\theta = 20°$, $\gamma_2 = 0$, $\gamma_3/\gamma_1 = 0.01$. (a):$\Psi = 18°$ (C1 state), (b):$\Psi = -18°$ (C2 state).

The normalized anchoring energies of the upper substrate f_s^d/γ_1^d are shown in Fig.2(a) for the C1 state, in Fig.2(b) for the C2 state, respectively. Here, $\theta = 20°$, $|\Psi| = 18°$, $\gamma_2 = 0$ and $\gamma_3/\gamma_1 = 0.01$. In the following, we fix $\gamma_3/\gamma_1 = 0.01$ because the anchoring strength of the in-plane tilt has known to be smaller than that of the out-of-plane tilt by the order of two in the case of nematic liquid crystals.[11)]

In the C1 state, the anchoring function has two stable angles that are symmetrically located about $\pi/2$. We denote these two states as R-state ($0 < \Phi_R^d < \pi/2$) and L-state ($\pi/2 < \Phi_L^d < \pi$). The potential barrier between R-state and L-state (at $\Phi^d = \pi/2$) is higher and the stable angles approaches 0 and $\pi/2$ as the pretilt angle β increases.

In the C2 state, the anchoring function has also two stable angles that are symmetrically located about $-\pi/2$ when $\beta < \theta - |\Psi|$. We denote these two states as R-state ($0 < |\Phi_R^d| < \pi/2$) and L-state ($\pi/2 < |\Phi_L^d| < \pi$). However, the anchoring function has only one minimum at $\Phi = -\pi/2$ when $\beta \geq \theta - |\Psi|$. We denote this state as O-state.

The anchoring energy of the lower substrate f_s^0/γ_1^0 has the same form if we replace Ψ by $-\Psi$ and Φ by $-\Phi$.

From eq.(12), it is found that there are always two stable states (R-state and L-state) at the chevron interface. In combination of the stable states at the upper substrate, the chevron interface and the lower substrate, there are eight possible states for the memory states of SSFLC cells, i.e., RRR, LLL, RRL, RLL, LRR, LRR, RLR and LRL-states, where the first, the second and the third capital letter indicate the state at the upper substrate, the chevron interface and the lower substrate, respectively. The RRR and LLL-states are known as uniform states (U-state) and RRL, RLL, LRR and LLR are known as half splayed states (T-state). The RLR and LRL may be called full splayed states. The bulk elastic energy of full splayed states is much higher than the U-states and the T-states. Therefore,

these states may not appear in the actual cases.

When $\beta \geq \theta - |\Psi|$ in the C2-state, however, only the O-state is allowed at the substrates. Therefore, only ORO and OLO states are possible. Because of the elastic torque, the O-states at the substrates deviate to R-states or L-states depending on the chevron state is R or L. Therefore, only the RRR and LLL states are stabilized. This is the reason why C2T does not appear in the cell with high pretilt aligning films.[12)]

3.2 *Polarization Reversal Current of C1 and C2 States*

Now let us investigate the switching characteristics of the C1 and C2-states under triangular wave voltages.

To solve the set of equations (15)-(19) and eq(21), we use the conventional difference method for the space Y and time t derivatives. The number of divisions along Y-axis is 40. The parameters used in the calculations are as follows; molecular tilt angle $\theta = 20°$, layer tilt angle $\Psi = 18°$, pretilt angle $\beta^d = -1°$(low pretilt) or $\beta^d = -5°$(high pretilt), cell thickness $d = 2\mu$m, spontaneous polarization $P_s = 5 \times 10^{-5}$C/m^2, rotational viscosity $\lambda = 5 \times 10^{-2}$Ns/m, dielectric constant $\varepsilon_2 = 5.65$, $B_1 = B_2 = 5 \times 10^{-11}$N and $B_3 = B_{13} = D = D_1 = 0$. The anchoring conditions are $\gamma_1 = 1 \times 10^{-2}$N/m, $\gamma_2 = 0$, $\gamma_3 = 0.01\gamma_1$ and $\gamma_c = 1.25 \times 10^{-3}$N/m. Here the dielectric anisotropy is neglected, *i.e.*, $\Delta\varepsilon = \partial\varepsilon = 0$.

Figures 3(a), 3(b), 3(c) and 3(d) shows the results for C1-state with $\beta = 1°$, for C2-state with $\beta = 1°$, for C1-state with $\beta = 5°$ and for C2-state with $\beta = 5°$, respectively. The amplitude and frequency of the triangular wave voltages are 20V and 100Hz. In each figure, the upper part shows the applied voltage and the polarization reversal current normalized by their maximum values, and the lower part shows the curves of equal azimuthal angle at steps of 10°.

In Fig.3(a) (C1-state with low surface pretilt), the polarization reversal current shows double peaks because the polarization reversals at the substrates are delayed with respect to that in the bulk and at the chevron interface.[5)] This is because γ_1 is much greater than γ_c. In Fig.3(b) (C2-state with low surface pretilt), however, single peaks appear because the potential barrier height between two stable points at the substrates in the C2-state is much lower than the case of the C1-state (see Fig.2) and the polarization reversal occurs almost uniformly over the cell. Also in Fig.3(c) (C1-state with high surface pretilt), the polarization reversal current shows single peaks. But the situation is different from Fig.3(b). The potential barrier height between two stable points at the substrates in this case is much higher than the case of Fig.3(a), and the polarization reversal cannot occur at the substrates. In the C2-state with high surface pretilt (Fig.3(d)), the polarization reversal current shows single peaks. The directors at the substrate only oscillate around $|\Phi| = 90°$ because the anchoring condition in this case is monostable as mentioned above.

3.3 *Effect of Dielectric Anisotropy on Switching*

Let us investigate the switching from the RRR-state to the LLL-state (uniform-

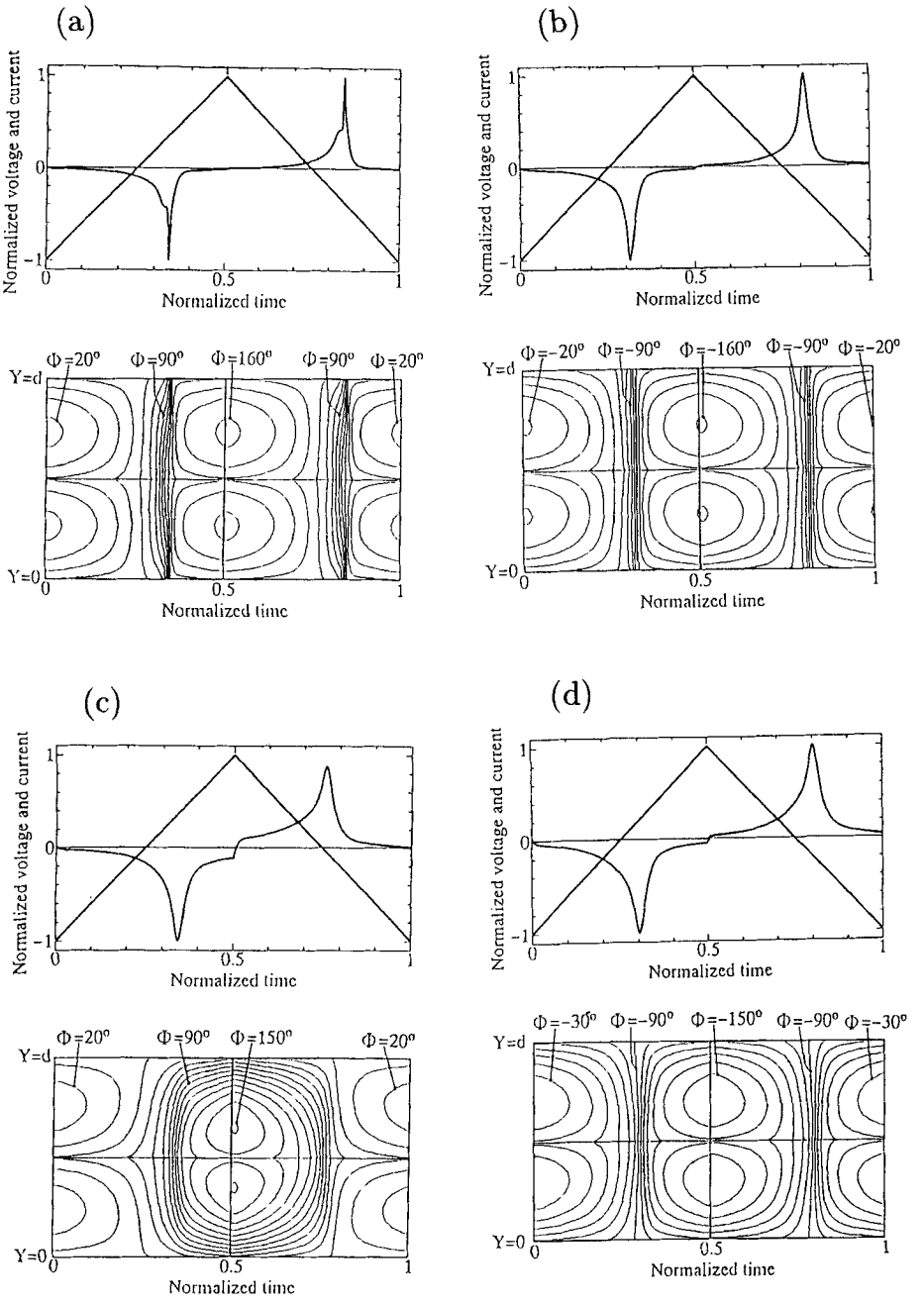

Fig.3 Applied triangular wave voltage and polarization reversal current normalized by their maximum values (upper figure) and curves of equal azimuthal angle (lower figure). (a):C1 state with low surface pretilt (1°), (b):C2 state with low surface pretilt (1°), (c):C1 state with high surface pretilt (5°), (d):C2 state with high surface pretilt (5°).

uniform switching) under a pulsed voltages. At a given pulse height, there exist a critical pulse width that is necessary for switching. When the dielectric anisotropies are neglected, this critical pulse width decreases monotonously as the pulse height increases. In particular, when the anchoring strength at the substrates and at the chevron interface are sufficiently weak, switching is almost uniform through the cell and the product of the pulse width and the pulse height that is necessary for switching is nearly constant.[6)]

On the other hand, it has been known that low P_s ferroelectric liquid crystals show a minimum in response time (τ) as a function of the applied voltages (V),[13)] due to electric field coupling to the dielectric anisotropy dominating the coupling to P_s at high voltages. Towler *et.al.* examined the minimum in $\tau - V$ curve as $\Delta\varepsilon$ and $\partial\varepsilon$ as parameters by the uniform switching case (the elastic torque is neglected).[14)] They showed that for a given $\Delta\varepsilon(< 0)$, $V_{\min}$ can be reduced by increasing $\partial\varepsilon$.

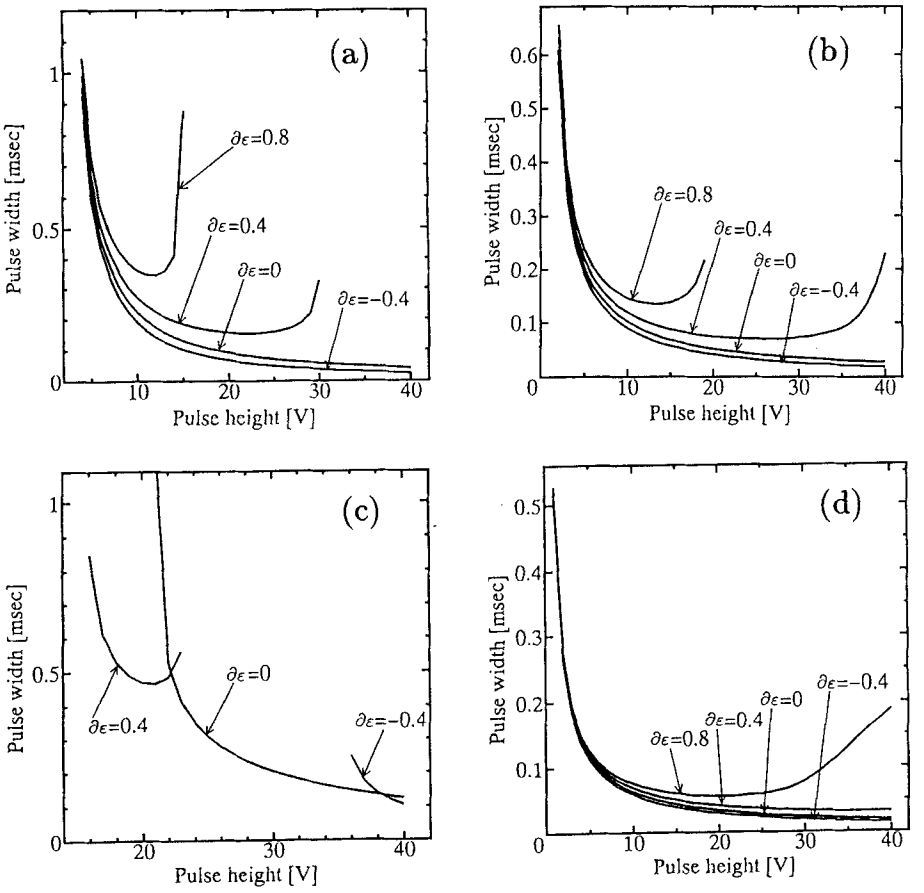

Fig.4 Critical pulse width that are necessary for switching as a function of pulse height ($\tau - V$ curve). (a):C1 state with low surface pretilt (1°), (b):C2 state with low surface pretilt (1°), (c):C1 state with high surface pretilt (5°), (d):C2 state with high surface pretilt (5°).

In this subsection, we investigate the effect of $\partial\varepsilon$ on switching in the C1 and C2 states by taking account of the elastic torque. The numerical calculation procedure and the numerical parameters are the same as those in the previous subsection.

The $\tau - V$ curves are shown in Fig.4 with $\partial\varepsilon$ as a parameter. We set $\Delta\varepsilon = 0$ because the effect of $\Delta\varepsilon$ is not so outstanding as that of $\partial\varepsilon$. Figures 4(a), 4(b), 4(c) and 4(d) shows the results for C1-state with $\beta = 1°$, for C2-state with $\beta = 1°$, for C1-state with $\beta = 5°$ and for C2-state with $\beta = 5°$, respectively.

From the comparison of the C1 states and C2 states (Fig.4(a) and 4(b), 4(c) and 4(d)), it is found that the critical pulse width is longer for the C1 states. This is because the potential barrier between two stable points at the substrate is higher for the C1 states. The critical pulse width is always longer as $\partial\varepsilon$ is larger in the case (a), (b) and (d). This is due to the fact that the dielectric free energy takes its minimum value at $\Phi = 0, \pi$ (see eqs.(7) and (8)), thus, the dielectric torque stabilizes the initial state.

From this view point, the results in Fig.4(c) might be rather curious at first sight, because the critical pulse width for $\partial\varepsilon = 0.4$ is shorter than that for $\partial\varepsilon = 0$ when $V < 23$V. Figure 5 explains the reason for this situation. Figure 5 shows the dynamic response of the azimuthal angle of the director at the upper substrate ($Y = d$), at just above the chevron interface ($Y = d/2$) and in the bulk ($Y = 3d/4$ as a representative of the bulk) under the same parameters with Fig.4(c) when a pulsed voltage with the pulse height of 20V and with the pulse width of 2ms is applied. In this case, the potential barrier between two stable points at the ssubstrate is considerably high, then, the switching at the substrates is hard to occur. Therefore, in the case of $\partial\varepsilon = 0$ (Fig.5(a)), the directors at the chevron

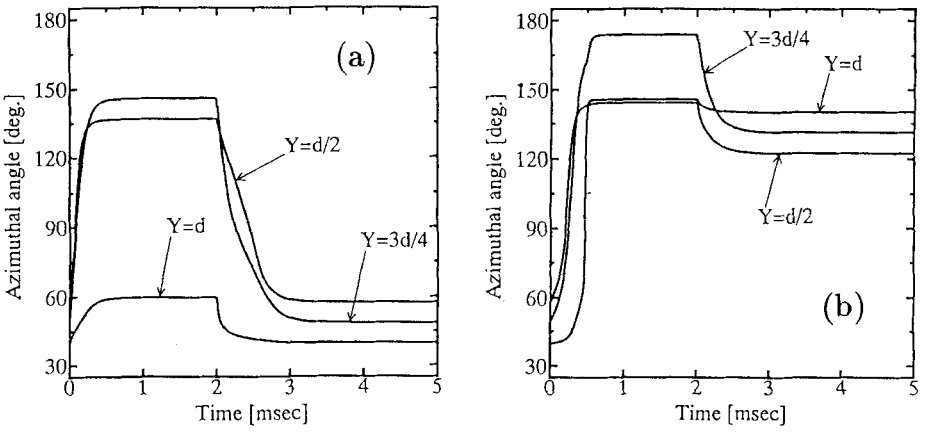

Fig.5 Transitional behavior of the azimuthal angle of the directors at the upper substrate ($Y = d$), at just above the chevron interface ($Y = d/2$) and in the bulk ($Y = 3d/4$) in the C1 state with high surface pretilt (5°) when a pulsed voltage with pulse height of 20V and with pulse width of 2ms is applied. (a):$\partial\varepsilon = 0$, (b):$\partial\varepsilon = 0.4$.

interface and in the bulk are once switched (the azimuthal angles once become greater than 90°), but the directors at the substrates cannot be switched. As a result, the directors at the chevron interface and in the bulk are pulled back by the elastic torque from the substrates. In the case of $\partial\varepsilon = 0.4$ (Fig.5(b)), however, once the azimuthal angles at the chevron interface and in the bulk become greater than 90°, the dielectric torque forces them to go toward 180°. As a result, the directors at the substrates are switched due to the elastic torque from the bulk. Therefore, the results in Fig.4(c) indicate the significance of the combined effect of the elastic torque and the dielectric torque.

4 Conclusion

The switching characteristics both of the C1 and C2 states in SSFLCs were investigated by means of simulations based on a model of SSFLC. In particular, the effects of surface anchoring conditions and dielectric anisotropy on them were studied. Main results are as follows;

1. When the polar surface anchoring is absent, in the C1 state, there always two stable azimuthal angles at the substrates which are symmetric with respect to $|\Phi| = 90°$. the potential barrier between two stable points is higher as the out-of-plane pretilt angle (β) is higher. In the C2 state, however, there is only one stable point ($|\Phi| = 90°$) when $\beta \geq \theta - |\Psi|$ where β, θ and Ψ are the out-of-plane pretilt angle, the molecular tilt angle and the layer tilt angle, respectively.

2. Switching of C2 state occurs with shorter pulse width and/or lower pulse height than that of C1 because the potential barrier between two stable point at the substrates is lower for the former.

3. The $\tau - V$ (the critical pulse width - pulse height) curves show a minimum due to dielectric anisotropy in accordance with the uniform switching theory by Towler *et.al.*[14)]

4. In general, the critical pulse width is longer as the biaxial dielectric anisotropy $\partial\varepsilon$ increases. Exceptions, however, exist due to the combined effect of the elastic torque and the dielectric torque.

In conclusion, the switching characteristics of SSFLC cells are profoundly affected by the surface anchoring conditions and dielectric anisotropies.

References

[1] T. P. Rieker, N. A. Clark, G. S. Smith, D. S. Parmar, E. B. Sirota and C. R. Safinia: Phys. Rev. Lett. **59**,2658(1987)

[2] N. A. Clark and T. P. Rieker: Phys. Rev. **A37**,1053(1988)

[3] J. Kanbe, H. Inoue, A. Mizutome, Y. Hanyuu, K. Katagiri and S. Yoshihara: Ferroelectrics, **114**,3(1991)

[4] N. Itoh, M. Koden, S. Miyoshi and T. Wada: Liquid Crystals, **15**, 669(1993).

[5] T. Akahane, K. Itoh and N. Nihei: Jpn. J. Appl.Phys. **32**,5041(1993)

[6] T. Anabuki, T. Sakonjuh, M. Kimura and T. Akahane: Ferroelectrics (1994) in press

[7] S. T. Lagerwall and I. Dahl: Ferroelectrics **58**, 215(1984).

[8] P. G. Amaya, M. A. Handschy and N. A. Clark: Opt. Eng. **23**, 261(1984).

[9] M. Nakagawa, M. Ishikawa and T. Akahane: Jpn. J. Appl. Phys. **27**, 456(1988).

[10] M. Nakagawa and T. Akahane: J. Phys. Soc. Jpn. **55**, 4429(1986).

[11] T. Sugiyama, S. Kuniyasu, D. Seo, H. Fukuro and S. Kobayashi: Jpn. J. Appl.Phys. **29**,2045(1990).

[12] N. Itoh, M. Koden, S. Miyoshi and T. Wada: Jpn.J. Appl.Phys., **31**, 852(1992).

[13] H. Orihara, K. Nakamura, Y. Ishibashi, Y. Yamada, N. Yamamoto and M. Yamawaki:Jpn.J. Appl.Phys., **25**, 839(1986).

[14] M. J. Towler, J. C. Jones and E. P. Raynes: Liquid Crystals, **11**, 365(1992).